View metadata, citation and similar papers at core.ac.uk

brought to you by CORE

provided by SocioEconomic Challenges Journal (Sumy State University)

PROCEEDINGS OF THE INTERNATIONAL CONFERENCE NANOMATERIALS: APPLICATIONS AND PROPERTIES
Vol. **1** No 3, 03TF14(4pp) (2012)

Analysis of the Electronic and Band-Structure in As-grown and Annealed (Ga,Mn)As Epitaxial Layers

O. Yastrubchak[1*], J. Sadowski[2,3], J. Z. Domagala[2], J. Żuk[1], T. Andrearczyk[2], and T. Wosiński[2]

[1] *Institute of Physics, Maria Curie-Skłodowska University in Lublin, Pl. Marii Curie-Skłodowskiej 1, 20-031 Lublin, Poland*
[2] *Institute of Physics, PAN, 02-668 Warsaw, Poland*
[3] *MAX-Lab, Lund University, 22100 Lund, Sweden*

(Received 18 June 2012; revised manuscript received 29 June 2012; published online15 July 2012)

The photoreflectance (PR) spectroscopy was applied to study the band-structure evolution in (Ga,Mn)As layers with increasing Mn content. We investigated (Ga,Mn)As layers and, as a reference, undoped GaAs layer, grown by LT-MBE on semi-insulating (001) GaAs substrates. Photoreflectance studies were supported by Raman spectroscopy and high resolution X-ray diffractometry (XRD) measurements. Magnetic properties of the (Ga,Mn)As films were characterized with a superconducting quantum interference device (SQUID) magnetometer. In addition, we investigated impact of the annealing of 100 nm (Ga,Mn)As layers with 6% of the Mn content on the electronic and band structure as well as on the electrical and magnetic properties of these films. Our findings were interpreted in terms of the model, which assumes that the mobile holes residing in the valence band of GaAs and the Fermi level position determined by the concentration of valence-band holes.

Keywords: (Ga,Mn)As, Diluted ferromagnetic semiconductor, Photoreflectance (PR) spectroscopy, Fermi level, Band-structure, Annealing.

PACS numbers: 71.20.Mq, 78.66.Fd

1. INTRODUCTION

(Ga,Mn)As has become a model diluted ferromagnetic semiconductor, in which a few percent of Ga lattice atoms have been substituted by Mn atoms. Below a magnetic transition temperature, T_c, substitutional Mn^{2+} ions are ferromagnetically ordered owing to interactions with spin-polarized mobile holes. Mn atoms substituting the Ga lattice sites in the LT-GaAs host, Mn_{Ga}, act as acceptors. This results in a high hole density, which is assumed to play a crucial role in the hole-mediated ordering of Mn spins. On the other hand, Mn atoms occupying interstitial sites of the crystal lattice, Mn_I, act as double donors in GaAs and, together with the native As_{Ga} donors, partially compensate Mn_{Ga} acceptors, thus resulting in effective reduction of the hole concentration in the (Ga,Mn)As films and, in turn, in decreasing their Curie temperature.

However, the character of electronic states near the Fermi energy and the valence-band structure in ferromagnetic (Ga,Mn)As are still a matter of controversy. There are two alternative models of the band structure in (Ga,Mn)As. The first one assumes mobile holes residing in the valence band of GaAs and the Fermi level position determined by the concentration of valence-band holes [1–3]. In this case the interband transition energy E_0 blue shifted with increasing of Mn content for insulator-like (Ga,Mn)As materials and red shifted for metallic-like (Ga,Mn)As epitaxial layers. The second one involves persistence of the narrow, Mn-related, impurity band in highly Mn-doped (Ga,Mn)As with metallic conduction [4–6]. In this model the Fermi level exists in the impurity band within the band gap, the mobile holes retain the impurity band character and interband transition energy blue shifted with increasing of Mn content in all type of (Ga,Mn)As epitaxial layers.

In the present paper we have applied photoreflectance (PR) spectroscopy to study the band-structure evolution in (Ga,Mn)As layers with increasing Mn content and annealing treatment. Conventional annealing treatment is the most popular way to increase the Curie temperature in the (Ga,Mn)As epitaxial layers [7]. This process usually performed at the temperature of 180º C in the nitrogen or the oxygen atmosphere and combined with other procedures: covering of the surface, nanostructuring et. ex [8,9,10,11]. In the recent publication the authors report about the highest $T_c = 200K$ observed in the annealed (Ga,Mn)As nanowire [12].

From the study presented in our previous paper we could conclude that the band and electronic structure as well as ferromagnetic properties of (Ga,Mn)As epitaxial layers grown with the LT-MBE are determined not only by the Mn concentration, but by the concentration of the defects arising during the low temperature growth as well [13]. By the removing one of these defects - interstitial Mn - with the adjusting of the parameters of LT (Ga,Mn)As-growth and post-growing annealing we could achieve the higher Curie temperature [14].

2. EXPERIMENTAL

2.1 Samples

We investigated as-grown 100–300nm thick (Ga,Mn)As layers, with Mn content from 1% to 6%, grown by means of the low-temperature molecular-beam epitaxy (LT-MBE) method at a temperature of 230°C on semi-insulating (001)-oriented GaAs substrates and, as a reference, undoped GaAs layer, grown by LT-MBE on semi-insulating (001) GaAs substrate. In addition, we investigated impact of the annealing

* yastrub@hektor.umcs.lublin.pl

 © 2012 Sumy State University

treatment n the electronic and band structure of 100 nm (Ga,Mn)As layers with 6% of the Mn content as well as on the electrical and magnetic properties of these films. The annealing treatment was performed at the temperature 180°C in the oxygen atmosphere during 60h.

2.2 SQUID characterization

The results of superconducting quantum interference device magnetometry applied to the (Ga,Mn)As layers, presented in Figs. 1*a*,*b* and ***c***, show that they all exhibit an in-plane easy axis of magnetization and well-defined hysteresis loops in their magnetization vs. magnetic field dependence. The as-grown layers displayed the T_c values in the range between 40 K and 60 K. After the annealing treatment T_c values as well as magnetic moment increases significantly (from 40 K to 70 K) for the 100 nm $Ga_{0.94}Mn_{0.06}As$ epitaxial layers (Fig. 1c).

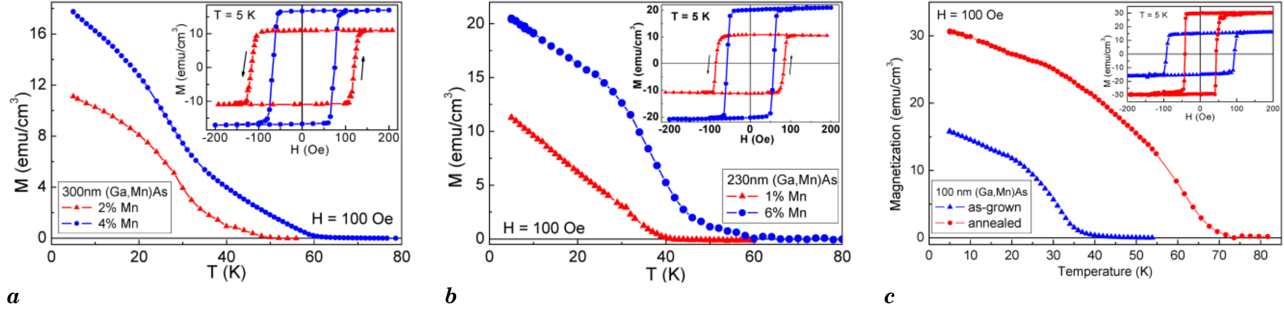

Fig. 1 – SQUID magnetization along the in-plane [110] crystallographic direction vs. temperature after subtraction of diamagnetic contribution from the GaAs substrates for two 300-nm-thick (Ga,Mn)As films with 2% and 4% of Mn content (***a***), two 230-nm-thick (Ga,Mn)As films with 1% and 6% of Mn content (***b***) and one 100-nm-thick (Ga,Mn)As layer with 6% of Mn content as-grown and annealed (***c***). Insets: magnetization hysteresis loops measured at a temperature of 5 K

2.3 Micro - Raman characterization

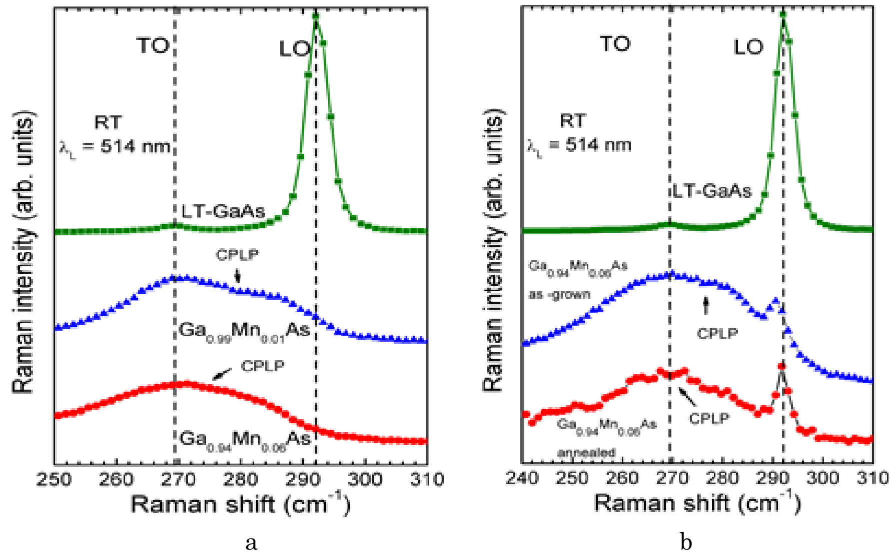

Fig. 2 – Micro-Raman spectra recorded using an "inVia Reflex" Raman microscope (Renishaw) at room temperature with the 514.5-nm argon ion laser line as an excitation source in backscattering configuration from the (001) surfaces of the LT-GaAs reference film and two 230-nm (Ga,Mn)As films with 1% and 6% of Mn content (***a***) and as-grown and annealed 100-nm (Ga,Mn)As films with 6% of Mn content (***b***). The spectra have been vertically offset for clarity. The dashed lines indicate the positions of the Raman LO- and TO-phonon lines for the LT-GaAs reference film and arrows indicate the position of CPLP mode

In (Ga,Mn)As films, characterized by a density of free holes of about 10^{20} cm^{-3}, the interaction between the hole plasmon and the LO phonon leads to the formation of coupled plasmon-LO-phonon (CPLP) mode [15,16]. In addition, it results in a broadening and a shift of the Raman line from the LO-phonon position to the TO-phonon position depending on the hole density [17].

By performing the analysis of our micro-Raman spectra obtained for the (Ga,Mn)As films, shown in Fig.2, we were able to estimate a hole concentration between 0.9×10^{20} cm^{-3} and 1.4×10^{20} cm^{-3} in the films with the Mn content from 1% to 6%, respectively (see Fig. 2a). These results suggest that the (Ga,Mn)As films with 1%-2% of Mn concentration demonstrates properties of an insulator-like material and the (Ga,Mn)As films with 3%-6% of Mn concentration - a metallic-like material. After the annealing treatment the free hole density increased in 100 nm $Ga_{0.94}Mn_{0.06}As$ epitaxial layer up to 1.6×10^{20} cm^{-3} (see Fig. 2b).

2.4 HR XRD — characterization

Our results of high-resolution XRD measurements performed for the as-grown and annealed films revealed that both the LT-GaAs and (Ga,Mn)As films were grown under compressive misfit stress and fully strained to the (001) GaAs substrate. The clear X-ray interference fringes, observed for the 004 Bragg reflections for the all heterostructures, indicate the high structural perfection of the films. Angular positions of the peaks corresponding to the LT-GaAs and (Ga,Mn)As films were used to estimate the strain of the epitaxial layers (see Fig. 3**)**. After the annealing treatment the strain of the 100 nm $Ga_{0.94}Mn_{0.06}As$ epitaxial layer decreased, probably because of decreasing the value of interstitial Mn atoms [14].

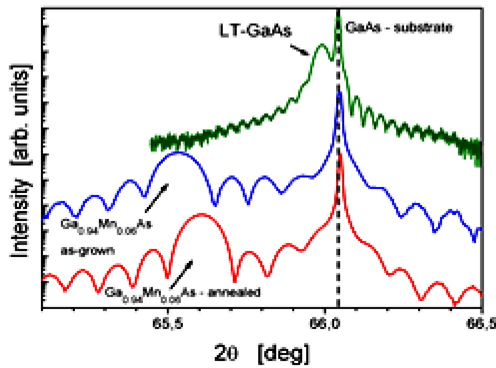

Fig. 3 – X-ray diffraction results: 2θ/ω scans for (004) Bragg reflections for 230-nm LT-GaAs and as-grown and 100 nm annealed $Ga_{0.94}Mn_{0.06}As$ thin films grown on (001) semi-insulating GaAs substrate. The curves have been vertically offset for clarity. The narrow line corresponds to reflection from the GaAs substrates and the broader peaks at lower angles (indicated with the arrows) are reflections from the epitaxial films. With increasing the Mn content the (Ga,Mn)As diffraction peaks shift to smaller angles with respect to that of the LT-GaAs reference film

2.5 Photoreflectance spectroscopy

The room temperature PR measurements were performed using semiconductor laser working at the 537 nm wavelength (penetration depth for GaAs - 150 nm) and a nominal power of 10-15 mW as a pump-beam source and a 250 W halogen lamp as a probe-beam source coupled to a monochromator. The PR spectra measured for LT–GaAs and (Ga,Mn)As epitaxial layers in the photon-energy range from 1.3 to 1.7 eV (Figs. 4a,b and Fig. 5) revealed a rich, modulated structures containing peaks (A) around the interband transition energy and electric-field-induced Franz-Keldysh oscillations (FKO) at energies above the fundamental absorption edge. The modulation mechanism of the feature around the interband transition energy results from the thermal excitation of impurities or traps at the (Ga,Mn)As/GaAs interface and their momentary refilling by the laser-injected carriers [19].

The energy values Eg connected with the interband transition energy E_0 are obtained from the intersection with the ordinate of the linear dependence of the energies of FKO extrema E_m vs. their “effective index” defined as $F_m = [3\pi(m - 1/2)/4]^{2/3}$:

$$E_m = E_g + \hbar\theta F_m \qquad (1),$$

where m is the extremum number and $\hbar\theta$ - the electro-optic energy defined as $\hbar\theta = \left(\frac{e^2\hbar^2F^2}{2\mu}\right)^{1/3}$, F is the electric field and μ is the interband reduced effective mass.

Because of the annealing treatment the Curie temperature as well as free hole concentration were significantly increased (Fig. **1*c*** and 2*b*) in 100 nm $Ga_{0.94}Mn_{0.06}As$ epitaxial layer. Nevertheless, the PR spectra for both as-grown and annealed heterostructures are very similar (Fig. 5*a*), the E_g energies does not changed significantly because of annealing treatment (Fig. 5*b*). The disordered-valence-band regime for high-Mn-doped (Ga,Mn)As predicted that the Mn-related impurity band and the host GaAs valence band merge into one inseparable band, whose tail may still contain localized states and Fermi level is located in the valence band, depending on the free carrier concentration and disorder. After the annealing treatment the interband transition energy was slightly blue shifted with respect to the as-grown (Ga,Mn)As. This was interpreted as a result of the Moss-Burstein shift of the absorption edge due to the Fermi level moving dipper into the valence band with the increasing free hole density as well as with the decreasing of the disorder and the compressive stress inside the annealed 100 nm $Ga_{0.94}Mn_{0.06}As$ epitaxial layer (see Fig. 3).

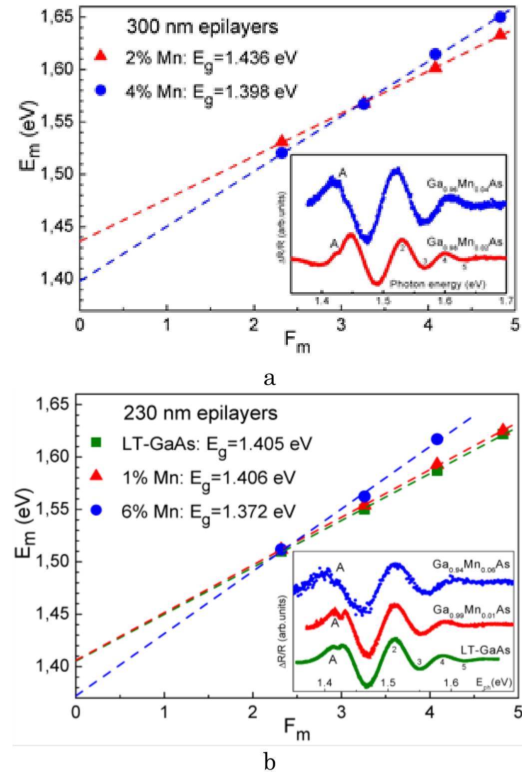

Fig. 4 – Analysis of the period of ranz-Keldysh oscillations for 300-nm $Ga_{0.98}Mn_{0.02}As$, and $Ga_{0.96}Mn_{0.04}As$ films (a) and 230-nm LT-GaAs, $Ga_{0.99}Mn_{0.01}As$, and $Ga_{0.94}Mn_{0.06}As$ films (b). Insets present the PR spectra for the 230-nm- and 300-nm-thick films where numbers of the FKO extrema used for the analysis are marked. The values of E_g obtained from the analysis are listed in the figures

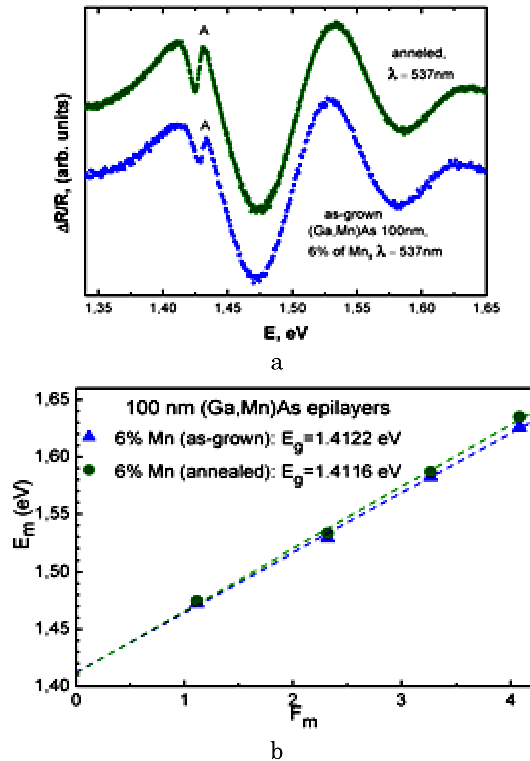

Fig. 5 – (a) Sequence of the photoreflectance spectra for the as-grown and annealed 100 nm $Ga_{0.94}Mn_{0.06}As$ film epitaxially grown on GaAs substrate (dots). The spectra have been vertically offset for clarity; (b) Analysis of the period of Franz-Keldysh oscillations for $Ga_{0.94}Mn_{0.06}As$ films shown in Fig. 5 (a). The values of E_g obtained from the analysis are listed in the figure

3. CONCLUSIONS

Our PR spectroscopy measurements enabled determination of the E_g electronic transition in (Ga,Mn)As epitaxial layers. In (Ga,Mn)As with a low (1–2%) Mn content and hole density close to that of the metal-insulator transition, the interband transition energy was blue shifted with respect to that in reference LT-GaAs, which was interpreted as a result of the Moss-Burstein shift of the absorption edge due to the Fermi level location below the top of GaAs valence band. On the other hand, a substantial red shift, of 40 meV, of the E_g energy was revealed in (Ga,Mn)As with the highest (6%) Mn content and a hole density corresponding to metallic side of the metal-insulator transition. This result, together with the determined other parameters of the intrerband electro-optic transitions near the center of the Brillouin zone, which were significantly different from those in reference LT-GaAs, was interpreted in terms of a disordered valence band, extended within the band-gap, formed in highly Mn-doped (Ga,Mn)As as a result of merging the Mn-related impurity band with the host GaAs valence band.

Annealing treatment does not impact significantly on the electronic and band-structure of (Ga,Mn)As epitaxial layers. Nevertheless, as a result of the annealing treatment, both the T_c and the free hole concentration increased significantly in the 100 nm $Ga_{0.94}Mn_{0.06}As$ epitaxial film. This behavior was connected with small increase of the E_g transition energy and degrease of the compressive strain in the layer.

ACKNOWLEDGEMENTS

O. Y. acknowledges financial support from the Foundation for Polish Science under Grant POMOST/2010-2/12 sponsored by the European Regional Development Fund, National Cohesion Strategy: Innovative Economy. This work was also supported by the Polish Ministry of Science and Higher Education under Grant No. N N202 129339.The MBE project at MAX-Lab is supported by the Swedish Research Council (VR).

REFERENCES

1. T. Dietl, H. Ohno, F. Matsukura, *Phys. Rev. B* **63**, 195205 (2001).
2. T. Jungwirth, J Sinova, J. Masek J. Kucera, A.H. MacDonald, *Rev. Mod. Phys.* **78**, 809 (2006).
3. M. Sawicki, D. Chiba, A. Korbecka, Y. Nishitani, J.A. Majewski, F. Matsukura, T. Dietl, H. Ohno, *Nature Phys.* **6**, 22 (2010).
4. K.S. Burch, D.B. Shrekenhamer, E.J. Singley, J. Stephens, B.L. Sheu, R.K. Kawakami, P. Schiffer, N. Samarth, D.D. Awschalom, D.N. Basov, *Phys. Rev. Lett.* **97**, 087208 (2006).
5. K. Alberi, K.M. Yu, P.R. Stone, O.D. Dubon, W. Walukiewicz, T. Wojtowicz, X. Liu, J.K. Furdyna, *Phys. Rev. B* **78**, 075201 (2008).
6. S. Ohya, I. Muneta, P.N. Hai, M. Tanaka, *Phys. Rev. Lett.* **104**, 167204 (2010).
7. M.B. Stone, K.C. Ku, S.J. Potashnik, B.L. Sheu, N. Samarth, P. Schiffer, *Appl. Phys. Lett.* **83**(22), 4568 (2003).
8. K.W. Edmonds, K.Y. Wang, R.P. Campion, A.C. Neumann, C.T. Foxon, B.L. Gallagher, P.C. Main, *Appl. Phys. Lett.* **81**(16), 3010 (2002).
9. B.J. Kirby, J.A. Borchers, J.J. Rhyne, S.G.E.T. Velthuis, A. Hoffmann, K.V. O'Donovan, T. Wojtowicz, X. Liu, W.L. Lim, Furdyna, *Phys. Rev.* B **69** (8), 081307 (2004).
10. K. Olejnik, M.H.S. Owen, V. Novak, J. Masek, A.C. Irvine, J. Wunderlich, T. Jungwirth , *Phys. Rev. B* **78**(5), 054403 (2008).
11. V. Stanciu, O. Wilhelmsson, U. Bexell, M. Adell, J. Sadowski, J. Kanski, P. Warnicke, P. Svedlindh, *Phys Rev B* **72** (12), 125324 (2005).
12. L. Chen, X. Yang, F.H. Yang, J.H. Zhao, J. Misuraca, P. Xiong, S. von Molnar, Nano Lett. **11**(7), 2584 (2011)
13. O. Yastrubchak, J. Zuk, H. Krzyzanowska, J.Z. Domagala, T. Andrearczyk, J Sadowski, T. Wosinski, *Phys. Rev. B* **83** (24), 245201 (2011)
14. J. Masek, J. Kudrnovsky, F. Maca, T. Jungwirth, *Acta Phys. Pol. A* **112** (2), 215 (2007)
15. M.J. Seong, S.H. Chun, H.M. Cheong, N. Samarth, and A. Mascarenhas, Phys. Rev. B **66**, 033202 (2002);
16. G. Irmer, M. Wenzel, and J. Monecke, *Phys. Rev. B* **56**, 9524 (1997);
17. W. Limmer, M. Glunk, W. Schoch, A. Köder, R. Kling, R. Sauer, and A. Waag, *Physica E* **13**, 589 (2002).
18. D.E. Aspnes and A.A. Studna, *Phys. Rev. B* **7**, 4605 (1973).
19. M. Sydor, J. Angelo, J.J. Wilson, W.C. Mitchel, and M.Y. Yen, *Phys. Rev. B* **40**, 8473 (1989).